

Title	Towards micropump- and microneedle-based drug delivery using Micro Transdermal Interface Platforms (MicroTIPs)
Authors	Tjulkins, Fjodors;Sebastian, Ryan;Guillerm, Theo;Clover, A. James P.;Hu, Yu;Lyness, Alexander;O'Mahony, Conor
Publication date	2022-07-15
Original Citation	Tjulkins, F., Sebastian, R., Guillerm, T., Clover, A. J. P., Hu, Y., Lyness, A. and O'Mahony, C. (2022) 'Towards Micropump- and Microneedle-based Drug Delivery using Micro Transdermal Interface Platforms (MicroTIPs)', 44th Annual International Conference of the IEEE Engineering in Medicine and Biology Society (IEEE EMBC 2022), Glasgow, Scotland, UK, 11-15 July, pp. 3020-3023. doi: 10.1109/EMBC48229.2022.9871455
Type of publication	Conference item
Link to publisher's version	<a href="https://doi.org/10.1109/EMBC48229.2022.9871455">https://doi.org/10.1109/EMBC48229.2022.9871455</a> - <a href="https://doi.org/10.1109/EMBC48229.2022.9871455">10.1109/EMBC48229.2022.9871455</a>
Rights	© 2022 The Authors. This work is licensed under a Creative Commons Attribution 3.0 License. For more information, see <a href="http://creativecommons.org/licenses/by/3.0/">http://creativecommons.org/licenses/by/3.0/</a> - <a href="http://creativecommons.org/licenses/by/3.0/">http://creativecommons.org/licenses/by/3.0/</a>
Download date	2025-03-22 00:27:32
Item downloaded from	<a href="https://hdl.handle.net/10468/13673">https://hdl.handle.net/10468/13673</a>



# UCC

**University College Cork, Ireland**  
Coláiste na hOllscoile Corcaigh

# Towards Micropump- and Microneedle-based Drug Delivery using Micro Transdermal Interface Platforms (MicroTIPs)

Fjodors Tjulkins, Ryan Sebastian, Theo Guillerm, A. James P. Clover, Yuan Hu, Alexander Lyness  
and Conor O'Mahony, *Senior Member, IEEE*

**Abstract—** Micro Transdermal Interface Platforms (MicroTIPs) will combine minimally invasive microneedle arrays with highly miniaturized sensors, actuators, control electronics, wireless communications and artificial intelligence. These patch-like devices will be capable of autonomous physiological monitoring and transdermal drug delivery, resulting in increased patient adherence and devolved healthcare.

In this paper, we experimentally demonstrate the feasibility of controlled transdermal drug delivery using a combination of 500  $\mu\text{m}$  tall silicon microneedles, a commercial micropump, pressure and flow sensors, and bespoke electronics. Using *ex-vivo* human skin samples and a customized application/retraction system, leak-free delivery of volumes ranging from 0.7-1.1 mL has been achieved in under one hour.

**Clinical Relevance—** This work experimentally confirms the feasibility of combining micropumps with microneedle arrays for applications in transdermal drug delivery.

## I. INTRODUCTION

As the prevalence of chronic diseases such as diabetes and auto-immune disorders continues to rapidly increase [1], it is imperative that the point of patient care is shifted from hospital to home in order to help alleviate the economic, social and epidemiological impacts of these conditions. Regular self-administration of therapeutics is essential for the efficient management of many such conditions, but the painful and inconvenient nature of self-injection regimens can often lead to very high levels of patient non-adherence. In turn, this may result in negative treatment outcomes and very large economic costs; the World Health Organisation (WHO) estimates that up to 50% of patients do not take medication as prescribed, and the cost of medication non-adherence is several hundred billion euro annually [2].

Needle-free, transdermal drug delivery (TDD) is an attractive route due to its painless nature, ease of administration, and lack of first-pass metabolism in the liver [3]. Microneedle technologies are the subject of immense interest for TDD, because of their ability to penetrate the skins outermost layer – the 10-20  $\mu\text{m}$  thick *stratum corneum* that is made up of cornified cells – and provide access to the 50-100  $\mu\text{m}$  thick viable epidermis that lies immediately beneath. Drugs and vaccines deposited here can diffuse towards the systemic circulation via the blood vessels found in the dermal

layer beneath, and administration of microneedle-based devices is perceived as painless by the user as the length and density of the needles is usually insufficient to strike the blood vessels or nerve endings that lie in the dermis.

Microneedles are sharp, needle-like structures that are generally several hundred microns tall, and made from a wide variety of materials ranging from silicon to polymers. Arrays of microneedles can be used in a variety of mechanisms: solid needles may be used to form transient micropores in the skin over which a topical medication is subsequently applied; needles may be coated with formulations into which an active ingredient is mixed; biodegradable microneedles are manufactured from a blend of water-soluble polymers and active ingredient; and hollow microneedles can infuse solutions directly into the skin through a narrow bore in the needle [4].

Infusion via hollow microneedles has the significant advantage of being controllable and, once skin-needle interface is reliably established, capable of delivering relatively large doses to the skin. While several studies have demonstrated the application of hollow microneedles in successful clinical trials [5], [6], manual use of hollow microneedle delivery devices generally requires the presence of trained clinical personnel and is not well suited to or self-administration. However, it ultimately will be possible to integrate these hollow microneedle arrays with microelectronic technologies such as miniaturized actuators, power sources, control electronics, embedded sensors and wireless communication protocols. The resultant microdosing platforms, that we refer to as Micro Transdermal Interface Platforms (MicroTIPs), will have patch-like form factors and will unobtrusively interact with the body without significant intervention from the patient themselves [7]. These platforms could dynamically and autonomously respond to conditions such as inputs from physiological sensors located either within the patch itself or elsewhere in or on the body, environmental and/or ambulatory conditions, remote clinical prescription, or as a result of alarm conditions generated during abnormal wear. MicroTIPs will have particular applications in the delivery of high-value drugs where adherence monitoring is of particular importance, such as biologics for the treatment of chronic conditions such as autoimmune disorders, diabetes or Parkinson's disease.

\* This work was supported by Enterprise Ireland and the ECSEL Joint Undertaking under grant number H2020-ECSEL-2019-IA-876190 (Moore4Medical), and by Enterprise Ireland and West Pharmaceutical Services under grant number IP2017/0560, and by the Science Foundation Ireland (SFI) Insight Centre for Data Analytics (SFI/12/RC/2289-P2).

F. Tjulkins, R. Sebastian, T. Guillerm, Y. Hu and C. O'Mahony are with the Tyndall National Institute, University College Cork, Ireland (e-mail: conor.omahony@tyndall.ie).

A. J. P. Clover is with the Dept. Plastic and Reconstructive Surgery, University College Cork, Cork, Ireland.

A. Lyness is with West Pharmaceutical Services, Exton, PA, USA.

Micropumps are miniaturized actuators capable of generating and controlling microfluidic flows; they have significant potential for use in microdosing applications [8]. Several academic groups have specifically investigated the merger of micropumps and microneedle arrays [9], [10], and a number of commercial suppliers are now providing micropumps that promise performance (e.g. maximum flowrates and pressures) and size characteristics approaching those required for use with wearable delivery devices such as MicroTIPs.

In this paper, we investigate the feasibility of deploying one such pump in microneedle-based transdermal drug delivery systems. By combining the pump with 500  $\mu\text{m}$  tall silicon microneedle arrays, pressure and flow sensors, and control electronics, leak-free delivery to *ex-vivo* human skin of volumes ranging from 0.7-1.1 mL has been achieved in under one hour. The data highlights the potential use of micropump-microneedle assemblies in wearable drug delivery systems.

## II. MATERIALS AND METHODS

### A. Microneedle Fabrication

Hollow silicon microneedle arrays were fabricated by firstly using potassium hydroxide (KOH) wet etching techniques to create solid structures, and a subsequent Deep Reactive Ion etch (DRIE) step to dry etch a bore through the needle [11], [12]. The starting material was boron doped, 100 mm diameter monocrystalline silicon wafers, orientated in the  $\langle 100 \rangle$  direction and onto which square oxide/nitride masks were patterned and aligned with the  $\langle 110 \rangle$  crystal direction using standard photolithography procedures. A solution of 29 % w/v aqueous KOH was used to etch the exposed silicon until convex corner undercutting took place and two planes formed at each corner. These eight planes subsequently intersected as the etch progressed, the mask detached, and a needle structure was formed.

After wet etch completion, a layer of aluminum was sputtered on the front side of the wafer to act as an etch stop, and capillary tubes were opened from the back side of the wafer using oxide/nitride hard masks and a dry etching tool (SPTS Technologies, Newport, UK) incorporating SF<sub>6</sub> and C<sub>4</sub>F<sub>8</sub> etch chemistries. The aluminum and masking layers were then stripped from both the front and rear sides of the wafer, respectively.

The resulting microneedles were in the shape of a 500  $\mu\text{m}$  tall octagonal cone, feature 71° sidewall angles, and had tip radii of the order of 50-100 nm. The crystal structure of the needle was comprised of eight {263} planes, a base of {212} planes and a height:base diameter aspect ratio of 3:2. The bore had a nominal diameter of 50  $\mu\text{m}$  and was positioned at a lateral offset of 50  $\mu\text{m}$  from the centre of the needle in order to preserve tip sharpness and avoid needle clogging during skin insertion.

A scanning electron microscope image of a 500  $\mu\text{m}$  tall hollow microneedle is shown in Figure 1. In this work, an array of three microneedles, spaced at a pitch of 1750  $\mu\text{m}$ , was used for skin infusion, Figure 2.

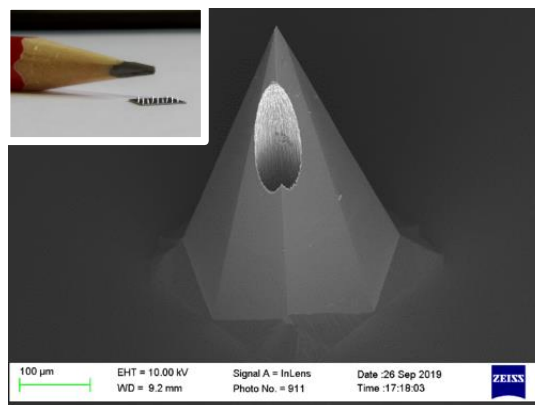


Figure 1. 500  $\mu\text{m}$  tall silicon microneedle. Inset: array of hollow microneedles.

### B. System Assembly

A commercial micropump (BCP-10E from Takasago Electric, Inc., Aichi, Japan) was used as the core of the system, Figure 2. This peristaltic pump measures 38.0 x 13.8 x 11.3 mm<sup>3</sup>, has a mass of 5g, a nominal standard flowrate of 50  $\mu\text{L}/\text{min}$  at zero backpressure, and a standard discharge pressure of 40 kPa, respectively. However, pump performance was seen to significantly exceed these specifications during infusion testing. The pump driving voltage is 1.5 to 2V [13].

For closed-loop control, an MS5837-30BA pressure sensor, (TE Connectivity, Schaffhausen, Switzerland) was used to measure fluidic pressure in the system. A commercial flow sensor (LD20-2600, Sensirion, Stafa, Switzerland) was used to measure the flowrate. Both pump and pressure sensor were interfaced to a custom PCB that included a low-power ESP32 microcontroller module (Espressif, Shanghai, China) and necessary discrete components. A step-down regulator Pololu 1.8V (Pololu, Las Vegas, USA) was used to power the pump at 1.8V.

The 3 x 1 microneedle array was glued to a 3D printed fitting, and fluidically connected to the micropump via the flow sensor using a 0.8 mm inner diameter tube. The pressure data was recorded using the microcontroller serial interface, and the flow data was recorded using a Sensirion USB to digital bus adapter and associated viewer software.

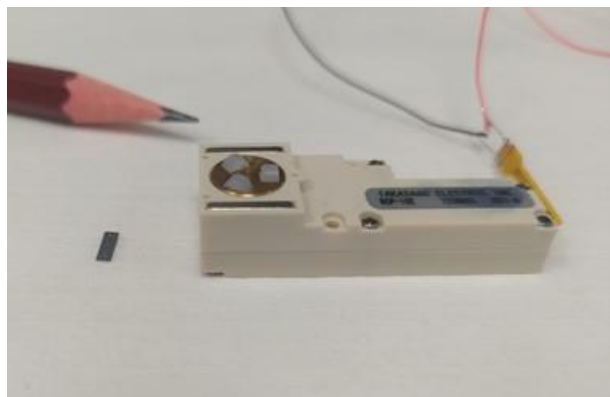


Figure 2. Takasago BCP-10E micropump, measuring 38 x 13.8 x 11.3 mm<sup>3</sup>, and weighing 5g (detachable head not shown). To the left of the pump is a 3 x 1 microneedle array.

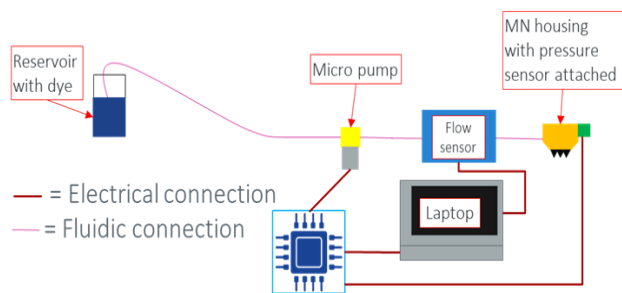


Figure 3. Experimental setup for skin infusion tests.

Data was analysed using Matlab, where flowrate was integrated over time to determine the total volume infused.

### C. Skin mounting and Needle Application

This study used *ex-vivo* human skin that was obtained following plastic surgical operations. Following protocols approved by the Clinical Research Ethics Committee of the Cork Teaching Hospitals (CREC) and informed consent from all patients, the skin was excised and stored at  $-80^{\circ}\text{C}$  until needed. It was then defrosted, trimmed of excess fat, and cut into pieces with approximate dimensions of  $35 \times 35 \text{ mm}^2$  and thickness of 3-4 mm after the removal of fat. Prior to use, the skin was incubated in PBS for 5 minutes at room temperature to replicate biological conditions.

The skin was mounted on a customized, 3D printed jig that incorporated a mechanical expansion mechanism. This allowed varying degrees of skin stretch to be achieved in a controlled manner, and a number of 1 mm thick plastic discs were also placed beneath the skin prior to stretching. In this manner, a lateral stretch of 3-4 mm and doming of the skin surface by 4-5 mm was achieved to replicate the surface shape that would be observed in *in-vivo* skin [14]. A fresh skin sample was used for each infusion.

A customized, spring-loaded applicator, with a spring constant of 274 N/m, was used to insert the needles in the skin. Previous studies have shown that the impact energy should be in the range of  $0.05\text{-}3 \text{ J/cm}^2$  [15]; in this work, an impact energy of  $2.9 \pm 0.1 \text{ J/cm}^2$  was used.

Other teams have also shown that optimal delivery via microneedles may be increased by periodically retracting the needle array, thereby avoiding skin compression and allowing skin expansion as the volume of infused fluid increases [16], [17]. This approach was also used here: the microneedle array was applied to the skin so that the needle tips were initially positioned  $1000 \mu\text{m}$  below the original location of the skin surface. This ‘compression depth’ was sufficient to embed the needles in the skin as well as generating a small residual spring force that aided in maintaining good skin-array contact.

The delivery protocol was based on pressure-driven flow: the pump was initially operated at full power for a period of five minutes, before being stopped. The pressure was then allowed to decay and tended to asymptotically approach a value of 5-20 kPa. A single needle retraction of  $100 \mu\text{m}$  was then performed, the pump was restarted until the system pressure peaked, and operation was maintained for a further three minutes afterwards. This decay-pump cycle was repeated a total of three times.

At all times a maximum gauge pressure of 100 kPa was set, and if this pressure was reached, then closed-loop modulation of the pump was used to maintain the 100 kPa level. However, the relatively low flow rate of the pump was comparable to the diffusion through the skin, and consequently the maximum pressure limit was often not reached. A solution of aqueous methylene blue dye was used as a model drug, which was passed through a  $0.45 \mu\text{m}$  filter before encountering the pump.

## III. RESULTS

Three tests were carried out, and the data is summarized in Table 1, below. Some variability is evident, which we attribute to the inherent variability associated with human skin, and to the difficulty in reliably achieving identical skin mounting conditions with each sample.

TABLE I. INFUSION VOLUME AND TEST TIME

Test	Infusion Volume (mL)	Time (min)
1	1.1	54.0
2	0.7	37.4
3	0.7	48.1

Commencement of a typical infusion test is shown in Figure 4. The pulsatile nature of the peristaltic flow is clearly visible; while the mean flowrate is approximately  $25 \mu\text{L}/\text{min}$ , instantaneous negative flow rates are also observed during each pumping cycle, which are due to the periodic compression and release of the pump tubing [18]. A full infusion cycle is shown in Figure 6. The target pressure setpoint of 100 kPa was frequently not reached, which we believe was due to the relatively low flow rate of the pump being matched or exceeded by diffusion of the fluid through the tissue. The pressure decreases rapidly following pump shutoff, indicating continuing diffusion through the skin is driven by the residual pressure in the system.

The maximum flowrate achieved by the pump was 70-90  $\mu\text{L}/\text{min}$ , significantly exceeding nominal values specified in the manufacturers datasheet.

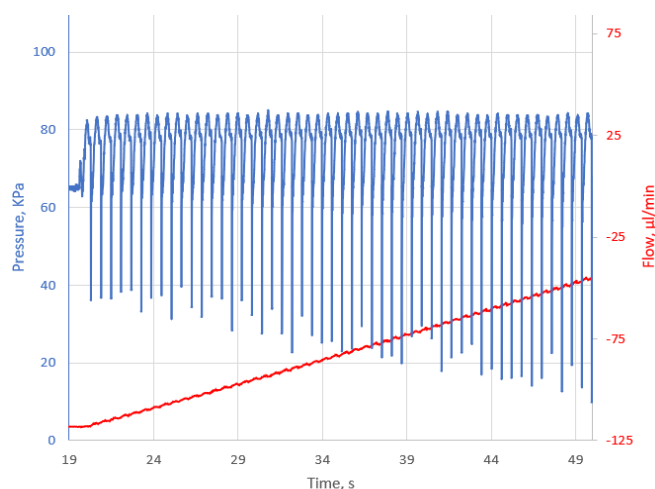


Figure 4. Pressure ramp-up and commencement of infusion.

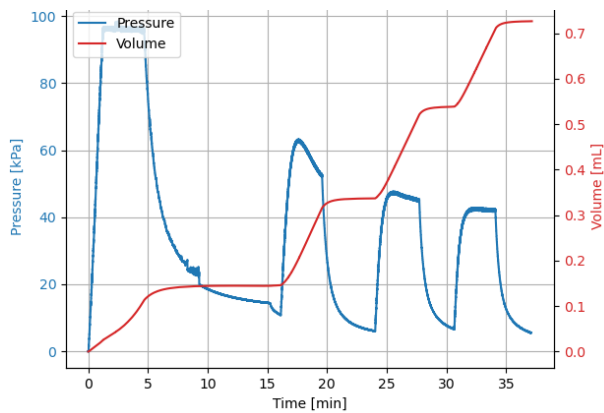


Figure 5. Cumulative volume as a function of delivery time. In this case, a total of 0.7  $\mu\text{L}$  was delivered over the 37.4 minute test. The needle retraction is visible at  $t=15$  minutes.

A skin sample held in the stretching jig and following delivery of 0.7 mL in 48 minutes is shown below, Figure 6. No leak was observed, and the imprint of the needle array and the three needles themselves are clearly visible after removal of the array. Diffusion of the methylene blue dye through the underlying skin layers is also evident.

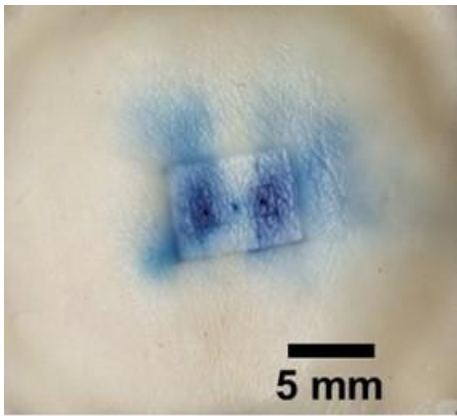


Figure 6. *Ex-vivo* human skin sample after the leak-free delivery of 0.8 mL in 48 minutes. The imprint of the microneedle array, and the epidermal diffusion of the dye is clearly visible beneath the surface of the skin.

#### IV. CONCLUSION

As a first step towards the autonomous theranostic wearables that we refer to as Micro Transdermal Interface Platforms ( $\mu\text{TIPs}$ ), we demonstrated the combined use of a commercial micropump and microneedle array for transdermal drug delivery. An application and retraction device was used in conjunction with a breadboard-level transdermal delivery system, consisting of a micropump, embedded sensors, microneedle array and control electronics.

Leak-free delivery rates of 0.9-1.2 mL/hour were achieved using a relatively small array of just three microneedles. The total infused volume could be increased further by using larger arrays, or by repeating pumping cycles at clinically relevant intervals.

Further work will continue to integrate and miniaturize the system, assess infusion protocols on delivery efficacy, and investigate the use of transdermal diagnostic sensors for closed-loop delivery. The study proves the feasibility of

delivering clinically relevant doses, over extended timescales, using minimally devices and actuators that could subsequently be integrated in wearable form factors.

#### ACKNOWLEDGMENT

The authors thank Tyndall's Specialty Products and Services team for microneedle processing.

#### REFERENCES

- [1] C. Hajat and E. Stein, "The global burden of multiple chronic conditions: A narrative review," *Preventive Medicine Reports*, vol. 12, pp. 284–293, Dec. 2018.
- [2] E. J. Unni, N. Sternbach, and A. Goren, "Using the Medication Adherence Reasons Scale (MAR-Scale) to identify the reasons for non-adherence across multiple disease conditions," *Patient Preference and Adherence*, vol. 13, pp. 993–1004, 2019.
- [3] W. Y. Jeong, M. Kwon, H. E. Choi, and K. S. Kim, "Recent advances in transdermal drug delivery systems: a review," *Biomaterials Research*, vol. 25, no. 1, p. 24, Dec. 2021.
- [4] T. Waghule *et al.*, "Microneedles: A smart approach and increasing potential for transdermal drug delivery system," *Biomedicine & Pharmacotherapy*, vol. 109, pp. 1249–1258, Jan. 2019.
- [5] P. Vescovo *et al.*, "Safety, tolerability and efficacy of intradermal rabies immunization with Debioject<sup>TM</sup>," *Vaccine*, vol. 35, no. 14, pp. 1782–1788, Mar. 2017.
- [6] Y. Levin, E. Kochba, I. Hung, and R. Kenney, "Intradermal vaccination using the novel microneedle device MicronJet600: Past, present, and future," *Human Vaccines & Immunotherapeutics*, vol. 11, no. 4, pp. 991–997, 2015.
- [7] C. O'Mahony *et al.*, "Embedded sensors for Micro Transdermal Interface Platforms (MicroTIPs)," in *2016 Symposium on Design, Test, Integration and Packaging of MEMS/MOEMS (DTIP)*, Budapest, Hungary, 2016, pp. 1–5.
- [8] A. B. Bußmann, L. M. Grünerbel, C. P. Durasiewicz, T. A. Thalhofer, A. Wille, and M. Richter, "Microdosing for drug delivery application—A review," *Sensors and Actuators A: Physical*, vol. 330, p. 112820, Oct. 2021.
- [9] R. Mishra, T. K. Maiti, and T. K. Bhattacharyya, "Feasibility Studies on Nafion Membrane Actuated Micropump Integrated With Hollow Microneedles for Insulin Delivery Device," *Journal of Microelectromechanical Systems*, vol. 28, no. 6, pp. 987–996, Dec. 2019.
- [10] F. Meshkinfam and G. Rizvi, "A MEMS-Based Drug Delivery Device With Integrated Microneedle Array—Design and Simulation," *Journal of Biomechanical Engineering*, vol. 143, no. 8, p. 081010, Aug. 2021.
- [11] N. Wilke and A. Morrissey, "Silicon microneedle formation using modified mask designs based on convex corner undercut," *Journal of micromechanics and microengineering*, vol. 17, no. 2, p. 238, 2007.
- [12] J. O'Brien *et al.*, "Hollow Microneedles for Pain-free Drug Delivery," presented at the Micromechanics Europe 2009, Toulouse, France, Sep. 2009.
- [13] *UltraSmall-Peristaltic Pump (Model: BCP-10E & TC-10E) USER'S MANUAL*, vol. UM-BCP10E\_REV. 0.03 (ENG). Takasago Electric, Inc., 2021.
- [14] D. Resnik *et al.*, "In Vivo Experimental Study of Noninvasive Insulin Microinjection through Hollow Si Microneedle Array," *Micromachines*, vol. 9, no. 1, p. 40, Jan. 2018.
- [15] J. C. Trautman, "Apparatus and method for piercing skin with microprotrusions," WO2006105272A2
- [16] P. Shrestha and B. Stoeber, "Fluid absorption by skin tissue during intradermal injections through hollow microneedles," *Scientific Reports*, vol. 8, no. 1, p. 13749, Dec. 2018.
- [17] P. M. Wang, M. Cornwell, J. Hill, and M. R. Prausnitz, "Precise Microinjection into Skin Using Hollow Microneedles," *Journal of Investigative Dermatology*, vol. 126, no. 5, pp. 1080–1087, May 2006.
- [18] M. Du, X. Ye, K. Wu, and Z. Zhou, "A peristaltic micro pump driven by a rotating motor with magnetically attracted steel balls," *Sensors (Basel)*, vol. 9, no. 4, pp. 2611–2620, 2009, doi: 10.3390/s90402611.